

A Single IRES Containing a G-quartet RNA Structure Drives FGF-2 Gene Expression at Four Alternative Translation Initiation Codons

Sophie Bonnal¹, Céline Schaeffer², Laurent Créancier^{1,3}, Simone Clamens¹, Hervé Moine², Anne-Catherine Prats¹ and Stéphan Vagner^{1,*}

¹INSERM U589, Institut Louis Bugnard, CHU Rangueil, 31403 Toulouse cedex 04, France;

²UPR 9002 CNRS, 67084 Strasbourg, France; ³Present address: Centre de recherche Pierre Fabre, 81106 Castres, France

*To whom all correspondence should be addressed; Tel : (33) 561 32 31 28 ; Fax : (33) 561 32 21 41. E-mail : vagner@toulouse.inserm.fr.

Running title: Structural determinants of the FGF-2 IRES

Key words : fibroblast growth factor 2, FGF-2, Internal ribosome entry site, IRES, translation

SUMMARY

The 484 nucleotides (nts)-long alternatively translated region (ATR) of the human fibroblast growth factor 2 (FGF-2) mRNA contains four CUG and one AUG translation initiation codons. While the 5'-end proximal CUG codon is initiated by a cap-dependent translation process, the other four initiation codons are initiated by a mechanism of internal entry of ribosomes. We undertook here a detailed analysis of the *cis*-acting elements defining the FGF-2 internal ribosome entry site (IRES). A thorough deletion analysis study within the 5' ATR led us to define a 176 nts-long region as being necessary and sufficient for IRES function at four codons present in a downstream 308 nts-long RNA segment. Unexpectedly, a single IRES module is therefore responsible for translation initiation at four distantly localized codons. The determination of the FGF-2 5' ATR RNA secondary structure by enzymatic and chemical probing experiments showed that the FGF-2 IRES contained two stem-loop regions and a G-quartet motif that constitute novel structural determinants of IRES function.

INTRODUCTION

The human FGF-2 gene belongs to a gene family of 23 fibroblast growth factors and is involved in various fundamental cellular processes, such as cell proliferation, differentiation and angiogenesis (1). The contribution of translational control in FGF-2 gene expression has been particularly well documented. First, a process of alternative initiation of translation occurs on the unique FGF-2 mRNA and leads to the production of five FGF-2 protein isoforms with extended NH2 terminal ends (2-4). Second, translation of four of these isoforms is initiated at non-canonical CUG codons (2-4). Third, the use of alternative initiation codons is controlled in transformed and stressed cells (5). Fourth, protein synthesis on the FGF-2 mRNA can occur by internal ribosome entry (6).

Whereas the usual mechanism of translation in eukaryotes involves the recruitment of the 40S ribosomal subunit to the 5' cap structure of the mRNA, a restricted but growing number of viral and cellular mRNA initiate their translation through the recruitment of the 40S ribosomal subunit to internal sequences of the mRNA called IRES (7-9). As regards the FGF-2 mRNA, this process is active *in vivo* in transgenic mice (10). Interestingly, the FGF-2 IRES is able to contribute to the choice of initiation codons since translation at the cap-proximal CUG codon occurs by a cap-dependent process whereas translation at the other four codons occurs by an IRES-based mechanism (4). To understand translation initiation codon selection in the FGF-2 mRNA, it is therefore important to define the *cis*-elements required for FGF-2 IRES function. The RNA sequences and structural features of cellular IRESs remain largely unknown. The various attempts to define the *cis*-acting elements required for the function of cellular IRES have failed to find a common RNA sequence. Cellular IRES appear to be very diverse in nature, without stringent sequence similarity. Since IRES elements in viral RNA genomes contain higher order structures whose integrities are essential for IRES activity, it was proposed that eukaryotic IRESs could also share some common RNA structural determinants. A Y-

shaped double hairpin RNA secondary structure was found in various cellular IRESs (11), although its functional role has never been clearly demonstrated. The only experimentally determined RNA secondary structure model of a cellular IRES revealed that the c-myc IRES contains a number of structural motifs including a pseudoknot helix, but not the predicted Y-shaped structure (12).

In this study, our goal was to determine the secondary structure of the FGF-2 5' ATR with chemical and enzymatic probing experiments and to precisely define the RNA sequences and structural determinants required for internal entry of ribosomes at each of the four IRES-dependent translation initiation codons. Our initial expectation, because of the reported modular nature of IRESs was that each of the initiation codons would be controlled by a distinct IRES element. A mutation and deletion study led us to show that a single IRES was able to control translation initiations at four downstream initiation codons in the FGF-2 mRNA. The FGF-2 IRES is 176-nucleotides long, is highly structured and contains two RNA stem-loops and a G-quartet motif each of these structural domains contributing to IRES activity.

EXPERIMENTAL PROCEDURES

Plasmid construction

Detailed information about DNA cloning procedures can be obtained from the authors upon request.

DNA transfection and luciferase activities

The SK-Hep 1 human hepatoma cell line was transfected with 1 ug of plasmid DNA per 60

mm tissue culture dishes with the Fugene-6 transfection reagent (Boehringer). Cell extracts were prepared 24 to 36 hours after transfection and analyzed for luciferase activities by using the Dual-Luciferase reporter assay system (Promega) as described in (13).

Structural-probing reactions on *in vitro* synthesized RNA

In vitro transcribed RNA (4 pmoles) was denatured for 1 min at 95°C and chilled on ice for 5 min. Incubation was continued for 10 min at 25°C following addition of the various reaction buffers (10mM Hepes-Na pH 7.5, 50 mM KCl, 2.5 mM MgCl₂ for RNAses T1 (Gibco) and V1 (Kemotex); 50 mM Na-borate pH 8.0, 50 mM KCl, 2.5 mM MgCl₂ for CMCT; 25 mM cacodylate-Na pH 7.5, 50 mM KCl, 2.5 mM MgCl₂ for DMS and kethoxal). Chemical modifications with DMS, CMCT and kethoxal were done during 5 min, 20 min and 15 min respectively in a 25 µl final volume as previously described (14). Enzymatic digestions were done with 0.05 units of RNase T1 or 0.0002 units of RNase V1 for 10 min at 25°C.

For primer extensions, the five different primers (RT75 5'-CCCACCAGCCTCCCGCGC-3' ; RT205 5'-CGCCGCCTGGGGAGAGCC-3' ; RT285 5'-CGCTCTTCTGTCCGCCGGC-3' ; RT365 5'-CCCGGCCCGGCCCGCC-3' ; RT445 5'-GGATCCCCGAGCCGCTGGA-3') were labeled with $\gamma^{32}\text{P}$ -ATP and combined with 2 pmoles of synthetic RNA. Hybridization and reverse transcription with the murine leukemia virus reverse transcriptase were carried out as described (14). The samples were analyzed on 8% polyacrylamide sequencing gels containing 8 M urea.

RESULTS

Secondary structure of the FGF-2 5' ATR

The secondary structure of the FGF-2 5' ATR RNA was determined by analyzing its enzymatic cleavage and chemical modification pattern obtained in native conditions in solution. The probing experiments were performed using an unlabelled *in vitro* transcribed RNA corresponding to the first 539 nucleotides of the human FGF-2 mRNA. We subjected this RNA to partial RNase digestions with RNAses T1 or V1. RNase T1 is known to cut 3' of G residues present in single-stranded regions, whereas RNase V1 cuts indicate doubled-stranded or stacked bases. We also used limited chemical modifications with three chemical probing agents, DMS, CMCT and kethoxal as described in experimental procedures. The sites of cleavage or modification were then identified by primer extension with reverse transcriptase, using various radiolabelled oligonucleotides complementary to five FGF-2 ATR sequences. Analysis of the resulting cDNAs was performed on sequencing polyacrylamide gels that were run together with the corresponding RNA sequencing ladder to allow identification of the modified residues. A typical example of the results is shown in figure 1.

A secondary structural model, presented in figure 2, was further derived by combining experimental data and free energy data calculated using the mFOLD program (15). The overall secondary structure of FGF-2 5' ATR appears as a succession of six independent stem-loop structures (labeled I to VI) (Fig. 2). The stem-loops are separated by short regions mostly single stranded (I to IV), or are directly adjacent (IV-VI). Due to the length and high GC content of their stems, these stem-loops are likely very stable, which is also indicated by the absence of reactivity towards the single strand specific probes and the numerous V1 cleavages within the stems. Some irregularities are present in the stems due to some bulged residues and internal loops. Some of these internal loops do possess some degree of order as indicated by the presence of RNase V1 cuts concomitant with single strand specific probes. This is re-

flecting the possible dynamic equilibrium between open and close conformation in these regions (e. g. region 194/216 and 305/348).

Within the FGF-2 5' ATR reactivity pattern, one region (involving nts 57-108) was particularly remarkable. Thus, this region was poorly reactive to probing while prediction structure programs failed to predict any structure involving it. The presence of strong pauses of reverse transcriptase progression immediately before this purine-rich region led us to test for the presence of an intramolecular purine-quartet. In a G quartet, the guanines are hydrogen bonded via Hoogsteen base pairs in a square-planar symmetric array and the quadruplex is stabilized by coordination of a monovalent K⁺ ion within the planes of the guanine tetrads (16). The formation and stability of G-quartets is cation-dependent with a preference for K⁺ over Na⁺ or Li⁺ (17). We therefore performed reverse transcriptase reactions with either KCl, NaCl or LiCl in the reaction buffer and found that stops of reverse transcriptase progression at positions U94, G101-102, U103, G104, A106 in KCl-containing buffer disappeared in NaCl- or LiCl-containing buffers (Fig 3A). Since the guanines in between positions 57 to 102 are neither accessible to RNase T1 digestion nor to DMS modification (position N1), we propose the presence of a G-quartet in this region (Fig. 3B).

Stem-loop II is critical for IRES activity at the CUG1 codon.

To analyze the elements of the FGF-2 5' ATR required for IRES activity, we used the bicistronic vector assay in which translation of the first cistron is cap-dependent and translation of the second cistron is IRES-dependent (7,8,18). Bicistronic mRNAs containing an upstream luciferase renillia (LucR) open reading frame (ORF) and a downstream luciferase firefly (LucF) ORF were expressed from plasmid vectors transfected into the SK-Hep1 human liver adenocarcinoma cell line, that was previously shown to harbor FGF-2 IRES activity (10).

To determine the elements required for IRES activity at each of the initiation codons, we used constructs in which the downstream LucF ORF was inserted either at the CUG1/320 (pCRFL1), CUG2/347 (pCRFL2), CUG3/362 (pCRFL3) or AUG/485 (pCRFL4) positions (Fig. 4). Moreover, to avoid LucF activity coming from upstream in-frame translation initiations, an in-frame UAG termination codon was inserted just upstream of AUG485 in the pCRFL4 plasmid and the CUG1 and/or CUG2 codons were mutated to non-initiating UUA codons in the pCRFL2 and pCRFL3 plasmids. Because in these vectors, the LucR activity reflects cap-dependent translation and is expected to be proportional to the amount of RNA produced whereas LucF activity measures the IRES activity, the LucF/LucR ratio gives the IRES activity normalized to the amount of RNA produced (10). Compared to the entire FGF-2 5'ATR in which the relative luciferase activity was set to an arbitrary value of 100% (pCRFL/100%), a control bicistronic vector that contains a short hairpin structure between the two cistrons functioned more than 10 times less efficiently in mediating second cistron translation (pCRHL/8%) (Fig. 4). The relative luciferase activity for plasmids pCRFL1 to pCRFL4 were between 59 and 69%, showing that an IRES activity can be measured at each of these four initiation codons. We therefore confirmed our previous observations (6) that four translation initiation codons on the FGF-2 mRNA can be selected by an internal ribosome entry process.

In order to localize the element(s) required for IRES activity at the CUG1 codon, we measured the relative luciferase efficiencies of a set of plasmid constructs containing various ATR deletions in the intercistronic space in the pCRFL1 background (Fig. 5A). The IRES activity at the CUG1 position was strongly reduced when the first 294 nucleotides of the FGF-2 5'ATR were deleted, indicating that the IRES is within this sequence. The IRES activity slightly decreased after deletion of domain III (Δ 177/221) (Fig. 5A). However, deletion of domains I (Δ 1/49), G4 (Δ 56/104) or of the single-stranded region between domains G4 and II

(Δ 105/126) decreased IRES activity at the CUG1 position (Fig. 5A). Furthermore, deletions of domains II and III together (Δ 127/221), domain II alone (Δ 127/176) or part of domain II (Δ 128/144) strongly decreased IRES activity at CUG1 (Fig.5A). We therefore concluded that various elements in domains I, G4 and II, but not in domain III, contribute to IRES activity and that a 17-nucleotides long region located within domain II, at positions 128-144 of the FGF-2 5' ATR, is the main element required for IRES activity at CUG1.

The same 17 nucleotides-long region in domain II is required for IRES-mediated translation at four downstream translation initiation codons

We next wondered whether nucleotides 128-144 of domain II would also be responsible for IRES activity at the CUG2 and CUG3 codons. In order to address this point, we deleted nucleotides 128 to 144 in the pCRFL2 and pCRFL3 background (Fig. 5B and 5C). The results showed that this deletion affected IRES activity at the CUG2 and CUG3 positions (Fig. 5B and 5C).

The same strategy was used to localize the element(s) required for IRES activity at the AUG/485 codon and various deletion constructs were made in the pCRFL4 background. As shown in Fig. 5D, deletions of the first 314, 338 or 377 nucleotides of the FGF-2 ATR strongly affected the IRES activity at the AUG showing that the elements required for IRES activity at this codon were not located in its close vicinity and might be present in the first 314 nucleotides of the FGF-2 ATR. Indeed, deletion of part of domain II (Δ 128/144) strongly decreased IRES activity at the AUG (Fig. 5D). Because the overall structure of the FGF-2 ATR, as determined by structural probing experiments, is not affected by deletion of stem-loop II (data not shown), we concluded that stem-loop II, located 308 nucleotides upstream of the AUG, is required for IRES activity at the AUG. Moreover, these data demonstrate that

the same features are necessary for IRES-mediated translation at four downstream initiation codons. The ability of the FGF-2 IRES to control translation initiation at four downstream codons was also observed in the Saos-2 osteosarcoma and SK-N-BE neuroblastoma cell lines that harbor strong FGF-2 IRES activity (10). Indeed, deletion of nucleotides 128 to 144 led to a 3 to 4 fold reduction in IRES activity in these cell lines (data not shown).

The integrity of stem-loop II is required for IRES activity

To test the structure of stem-loop II more thoroughly, we generated deletions and mutations in this region in the context of bicistronic luciferase construct pCRFL1. We first mutagenized the loop structure of stem-loop II. Deletion (Δ 141/152) or mutation (M142/150) of loop II led to a strong reduction in IRES activity (Fig. 6). We next mutagenized a 9 nucleotides-long sequence (from position 132 to 140) that was identical to a region present in the Gtx 5' UTR shown to mediate an interaction with the 18S ribosomal RNA (19) and internal entry of ribosomes (20). However, mutation of this sequence in the FGF-2 context (M132/140) did not affect IRES activity (Fig. 6). Mutation of the other side of the stem (M156/160) had no consequences on IRES activity (Fig. 6). Altogether, these data show that the loop sequence in stem-loop II is required for IRES activity.

A 176 nucleotides-long RNA module is sufficient to confer IRES activity

In order to determine whether stem-loop II was sufficient to mediate internal entry of ribosomes, we tested the IRES activity of a construct that contained domain II from positions 126 to 176 (pCRFL1 126/176). Because this activity was very weak, compared to the pCRFL1 parental construct (Fig. 7), we concluded that stem-loop II cannot function on its own as an

IRES. Surrounding sequences were then progressively added to find the minimal FGF-2 IRES sequence. The IRES activity of a construct that contained sequences normally located downstream of stem-loop II (pCRFL1 Δ 1/126) was still very weak, showing that sequences downstream of residue 176 are dispensable for IRES function. Contrarily, we found that constructs containing sequences normally located upstream of stem-loop II (pCRFL1 1/176 or pCRFL4 1/176) gave strong IRES activities that were very close to the parental constructs (pCRFL1 or pCRFL4) (Fig. 7A and 7B). Deletion of stem-loop I alone (pCRFL1 50/176), stem-loop I and half of the G4 domain together (pCRFL1 76/176 or pCRFL4 76/176) or stem-loop II alone (pCRFL1 1/126 or pCRFL4 1/126) in this 176 nts-long fragment reduced IRES activity. We therefore concluded that a 176 nucleotides-long sequence is necessary and sufficient for IRES activity.

DISCUSSION

We report here the RNA sequence and structural determinants of the FGF-2 IRES. Contrarily to other cellular IRES in which the IRES has been localized and shown to function in a modular fashion, with each module able to contribute singly to IRES activity (12,21,22), the FGF-2 IRES contains a single module. This module is 176 nts-long and is composed of two stem-loops and a G-quartet motif.

Studying the process of internal entry of ribosomes on the alternatively translated FGF-2 mRNA therefore allowed us to define novel structural determinants of IRES function. Strikingly, none of the known RNA features involved in IRES function are present in the FGF-2 IRES module. For instance, the FGF-2 IRES lacks a polypyrimidine tract required for IRES function of several cellular IRESs (23-25). The FGF-2 IRES contains a 9 nts-long sequence that is also present in the Gtx IRES and that functions on its own as an IRES (20). However,

mutation of these 9 nucleotides in the FGF-2 context did not impair internal entry of ribosomes. Several higher-order structures are also involved in IRES function. For instance, pseudoknot structures were shown to be required in various IRES (12,26-28). Furthermore, stem-loop structures containing a GNRA motif are shared by several picornavirus IRESs (29,30) and could be involved in RNA-RNA tertiary interactions. We could not find any evidences of the existence of such structures in loops I and II of the FGF-2 IRES. The lack of similarities between the FGF-2 IRES and other cellular or viral IRES could therefore reflect its unique property to be regulated at given physiological conditions by specific IRES *trans*-acting factors (ITAF). Indeed we have recently shown that the FGF-2 IRES does not require some of the classical ITAF such as hnRNP I/PTB and La autoantigen but instead we have demonstrated the role of hnRNP A1 as a novel ITAF for FGF-2 mediated translation (Bonnal et al., submitted). More generally, since a wide variety of nucleotide sequences seem to function as IRES and several proteins were identified as ITAF, the mechanisms by which translation preinitiation complexes are recruited to IRES-containing mRNA are likely to be different and should provide several targets for translational regulation of gene expression.

Interestingly, we have also found in this study that the FGF-2 IRES contains an intramolecular G quartet motif. Such motif has never been described in IRES sequences. It was found in several mRNAs that are bound by the fragile X mental retardation protein (FMRP) (31-33). The FGF-2 G-quartet motif contributes to IRES activity and may therefore behave as a positive translational element. This is surprising given the reported role of purine-quartet motifs in translation repression (34). Interestingly, the inefficient translation initiation at the cap-proximal CUG0 codon (4) may be explained by its localization within the G-quartet. The binding of FMRP or other proteins to the FGF-2 G-quartet motif and the role of these interactions in IRES-mediated translation await investigation.

Finally, we report here the relative position of an IRES and of alternative translation start sites. Although IRESs have been shown to be present in many mRNAs that contain a single translation initiation codon, their existence has been demonstrated on several mRNAs containing alternative initiation codons. The logical expectation is that IRESs present in alternative translation initiation systems contribute to the selection of the cap-distal internal codon whereas the cap-proximal codon is selected by a cap-dependent mechanism. This is indeed the case for the FGF-2 mRNA in which translation initiation at the 5'-end proximal CUG codon occurs by a cap-dependent mechanism whereas translation at the four downstream initiation codons occurs by an internal ribosome entry process (4). We provide evidence in this study that the position of the IRES overlapping the cap-proximal codon but upstream of the internal codons may explain this fact. This situation has also been found in the Moloney murine leukemia virus gag mRNA, the human VEGF mRNA or the human PITSLRE mRNA in which an IRES is present between two translation initiation codons and leads to the selection of the internal codon, thereby contributing to the control of alternative initiation of translation (13,35,36).

Conversely, IRESs can also be found upstream from several translation initiation codons without an apparent contribution to the selection of the alternative initiation codon. This situation is encountered in the FMDV (37), the c-myc (38,39), the Bag-1 (40), the VEGF (13) and the FGF-2 mRNAs. As regards the FGF-2 mRNA, a single IRES controls initiations at four downstream translation initiation codons located in a 308 nts-long RNA segment. Following the first step of internal entry of ribosomes that is determined by sequences present in the first 176 nts of the FGF-2 mRNA, the molecular events that will contribute to the selection of the four downstream initiation codons remain to be determined. Since the FGF-2 5' leader is highly structured, a "leaky scanning" mechanism is very unlikely (41). Although a ribosomal shunt mechanism (42) may account for selection of the four IRES-dependent

translation initiation codons present in the human FGF-2 mRNA, we favor a model in which the choice of alternative initiation codons depending on a single IRES will result from alternative RNA conformations, controlled by *trans*-acting factors, that will in turn favor ribosome recruitment at each of the alternative initiation codon.

ACKNOWLEDGEMENTS

This work was supported by INSERM, European commission (FP5, QoL Cell Factory, contract QLRT-2000-00721), ARC (“Association pour la Recherche sur le Cancer”) and by the French ministry of research (Action Concertée Incitative « Jeunes chercheurs »). S.B. is a recipient of an ARC pre-doctoral fellowship.

REFERENCES

1. Bikfalvi, A., Klein, S., Pintucci, G., and Rifkin, D. B. (1997) *Endocr Rev* 18, 26-45
2. Florkiewicz, R. Z., and Sommer, A. (1989) *Proc Natl Acad Sci U S A* 86, 3978-3981
3. Prats, H., Kaghad, M., Prats, A. C., Klagsbrun, M., Lelias, J. M., Liauzun, P., Chalon, P., Tauber, J. P., Amalric, F., Smith, J. A., and et al. (1989) *Proc Natl Acad Sci U S A* 86, 1836-1840
4. Arnaud, E., Touriol, C., Boutonnet, C., Gensac, M. C., Vagner, S., Prats, H., and Prats, A. C. (1999) *Mol Cell Biol* 19, 505-514
5. Vagner, S., Touriol, C., Galy, B., Audigier, S., Gensac, M. C., Amalric, F., Bayard, F., Prats, H., and Prats, A. C. (1996) *J Cell Biol* 135, 1391-1402
6. Vagner, S., Gensac, M. C., Maret, A., Bayard, F., Amalric, F., Prats, H., and Prats, A. C. (1995) *Mol Cell Biol* 15, 35-44
7. Hellen, C. U., and Sarnow, P. (2001) *Genes Dev* 15, 1593-1612
8. Vagner, S., Galy, B., and Pyronnet, S. (2001) *EMBO Rep* 2, 893-898
9. Bonnal, S., Boutonnet, C., Prado-Lourenco, L., and Vagner, S. (2003) *Nucleic Acids Res* 31, 427-428
10. Creancier, L., Morello, D., Mercier, P., and Prats, A. C. (2000) *J Cell Biol* 150, 275-281
11. Le, S. Y., and Maizel, J. V., Jr. (1997) *Nucleic Acids Res* 25, 362-369
12. Le Quesne, J. P., Stoneley, M., Fraser, G. A., and Willis, A. E. (2001) *J Mol Biol* 310, 111-126
13. Huez, I., Creancier, L., Audigier, S., Gensac, M. C., Prats, A. C., and Prats, H. (1998) *Mol Cell Biol* 18, 6178-6190
14. Brunel, C., and Romby, P. (2000) *Methods Enzymol* 318, 3-21
15. Zuker, M., Jaeger, J. A., and Turner, D. H. (1991) *Nucleic Acids Res* 19, 2707-2714

16. Laughlan, G., Murchie, A. I., Norman, D. G., Moore, M. H., Moody, P. C., Lilley, D. M., and Luisi, B. (1994) *Science* 265, 520-524
17. Sundquist, W. I., and Klug, A. (1989) *Nature* 342, 825-829
18. Sachs, A. B. (2000) *Cell* 101, 243-245
19. Hu, M. C., Tranque, P., Edelman, G. M., and Mauro, V. P. (1999) *Proc Natl Acad Sci U S A* 96, 1339-1344
20. Chappell, S. A., Edelman, G. M., and Mauro, V. P. (2000) *Proc Natl Acad Sci U S A* 97, 1536-1541
21. Yang, Q., and Sarnow, P. (1997) *Nucleic Acids Res* 25, 2800-2807
22. Sella, O., Gerlitz, G., Le, S. Y., and Elroy-Stein, O. (1999) *Mol Cell Biol* 19, 5429-5440
23. Holcik, M., Lefebvre, C., Yeh, C., Chow, T., and Korneluk, R. G. (1999) *Nat Cell Biol* 1, 190-192
24. Pyronnet, S., Pradayrol, L., and Sonenberg, N. (2000) *Mol Cell* 5, 607-616
25. Hudder, A., and Werner, R. (2000) *J Biol Chem* 275, 34586-34591
26. Wang, C., Le, S. Y., Ali, N., and Siddiqui, A. (1995) *Rna* 1, 526-537
27. Wilson, J. E., Powell, M. J., Hoover, S. E., and Sarnow, P. (2000) *Mol Cell Biol* 20, 4990-4999
28. Kanamori, Y., and Nakashima, N. (2001) *Rna* 7, 266-274
29. Robertson, M. E., Seamons, R. A., and Belsham, G. J. (1999) *Rna* 5, 1167-1179
30. Martinez-Salas, E., Quinto, S. L., Ramos, R., and Fernandez-Miragall, O. (2002) *Biochimie* 84, 755-763
31. Darnell, J. C., Jensen, K. B., Jin, P., Brown, V., Warren, S. T., and Darnell, R. B. (2001) *Cell* 107, 489-499

32. Schaeffer, C., Bardoni, B., Mandel, J. L., Ehresmann, B., Ehresmann, C., and Moine, H. (2001) *Embo J* 20, 4803-4813
33. Miyashiro, K. Y., Beckel-Mitchener, A., Purk, T. P., Becker, K. G., Barret, T., Liu, L., Carbonetto, S., Weiler, I. J., Greenough, W. T., and Eberwine, J. (2003) *Neuron* 37, 417-431
34. Oliver, A. W., Bogdarina, I., Schroeder, E., Taylor, I. A., and Kneale, G. G. (2000) *J Mol Biol* 301, 575-584
35. Vagner, S., Waysbort, A., Marena, M., Gensac, M. C., Amalric, F., and Prats, A. C. (1995) *J Biol Chem* 270, 20376-20383
36. Cornelis, S., Bruynooghe, Y., Denecker, G., Van Huffel, S., Tinton, S., and Beyaert, R. (2000) *Mol Cell* 5, 597-605
37. Belsham, G. J. (1992) *Embo J* 11, 1105-1110
38. Nanbru, C., Lafon, I., Audigier, S., Gensac, M. C., Vagner, S., Huez, G., and Prats, A. C. (1997) *J Biol Chem* 272, 32061-32066
39. Nanbru, C., Prats, A. C., Droogmans, L., Defrance, P., Huez, G., and Kruys, V. (2001) *Oncogene* 20, 4270-4280
40. Coldwell, M. J., deSchoolmeester, M. L., Fraser, G. A., Pickering, B. M., Packham, G., and Willis, A. E. (2001) *Oncogene* 20, 4095-4100
41. Kozak, M. (2002) *Gene* 299, 1-34
42. Ryabova, L. A., Pooggin, M. M., and Hohn, T. (2002) *Prog Nucleic Acid Res Mol Biol* 72, 1-39

FIGURE LEGENDS

Figure 1 : Enzymatic (panel A) and chemical (panel B) probing of *in vitro* transcribed FGF-2 5' ATR. Cleavage and modification sites were detected by primer extension using the ^{32}P -5' end-labelled RT285 oligonucleotide that hybridizes at position 285 to 303 of the FGF-2 RNA. The resulting cDNA was separated on 8% polyacrylamide/8 M urea sequencing gel and analyzed by autoradiography. RNA sequencing reactions were run in parallel. The nature and positions of cleaved (panel A) and modified (panel B) bases are indicated on the right side of each panel. RNase V1 (V1), RNase T1 (T1), or the three chemical agents (DMS, CMCT or Kethoxal) were added (lane +) or not (lane -) prior to the reverse transcription step.

Figure 2 : RNA secondary structure model of the FGF-2 5' ATR showing results from enzymatic cleavage and chemical modifications experiments. Domains I to VI are indicated as well as the G quartet motif (G4). White and black arrows represent weak-moderate and strong RNase T1 cleavage sites respectively. White and black triangles represent weak-moderate and strong RNase V1 cleavage sites respectively. Dashed, white and black circles represent weak, moderate and strong modifications by DMS, CMCT or kethoxal respectively. x marks represent reverse transcriptase pauses, with those that are cation-dependent boxed. Lower case letters are positions with non determined reactivity. Translation initiation codons are boxed.

Figure 3 : The FGF-2 G quartet motif. (A) Cation-dependent termination of reverse transcriptase at positions 94 to 106 of the FGF-2 5' ATR. Reverse transcriptase reactions were performed in presence of 100mM KCl (lane 5), 100 mM NaCl (lane 6) or 100 mM LiCl (lane 7) and were run together with RNA sequencing reactions (lanes 1 to 4). Strong pauses are indicated by asteriks whereas the full-length extension product is marked with an open triangle. (B) Schematic model of the FGF-2 G-quartet motif. Lanes between guanine bases represent the Hoogsteen interactions that occur in a square-planar symmetric array

Figure 4 : Schematic representation of bicistronic FGF-2 RNAs and their efficiency in directing internal entry of ribosome. The five translation initiation codons, their mutation to non-initiation UUA codons in the pCRFL2 and pCRFL3 constructs and the insertion of a UAG stop codon in the pCRFL 4 construct are shown. Relative luciferase activity is the LucF/LucR ratio in transiently transfected SK-Hep1 cells. The average relative luciferase activity was calculated from at least six experiments. An arbitrary value of 100 was set for the pCRFL construct. The pCRHL construct contains a 38 nts-long intercistronic spacer, as described in (10).

Figure 5 : Mapping the domains required for IRES-mediated translation at each of the FGF-2 translation initiation codons. A schematic representation of the FGF-2 5' leader RNA and the position of the structural domains I to III and G4 (see figure 4) are shown. Relative luciferase activities were calculated for each of deletion constructs transiently transfected in SK-Hep1 cells from at least four independent experiments performed in duplicate. An arbitrary value of 100 was set for the pCRFL1 construct in panel A, for pCRFL2 in panel B, for pCRFL3 in panel C and for pCRFL4 in panel D.

Figure 6 : Analyzing the requirements for FGF-2 IRES-mediated translation in stem-loop II. Schematic representation of the wild type stem-loop II and of the different mutants. Wild type nucleotides in the loop are in gray characters whereas mutated nucleotides are in bold

characters. The mutants were constructed in the pCRFL1 plasmid. The values for the average relative luciferase activities in transiently transfected SK-Hep 1 cells are shown at the bottom and were calculated from at least four experiments performed in duplicate. An arbitrary value of 100 was set for the parental pCRFL1 plasmid .

Figure 7 : Mapping the domains sufficient for IRES-mediated translation. The various constructs were transfected in SK-Hep1 cells and the average relative luciferase activities were calculated from three independent experiments performed in duplicate.

Figure 1, Bonnal et al.

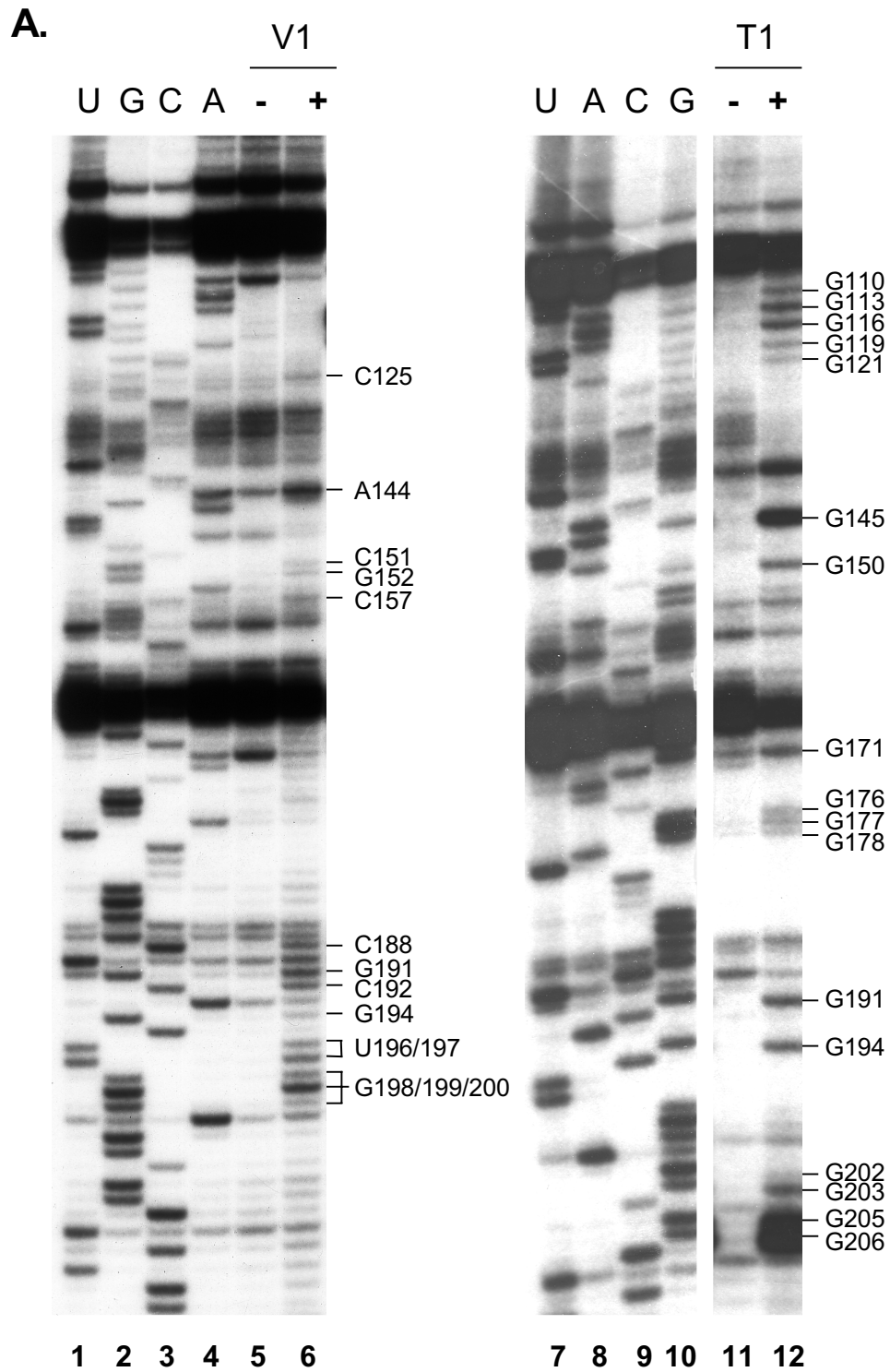
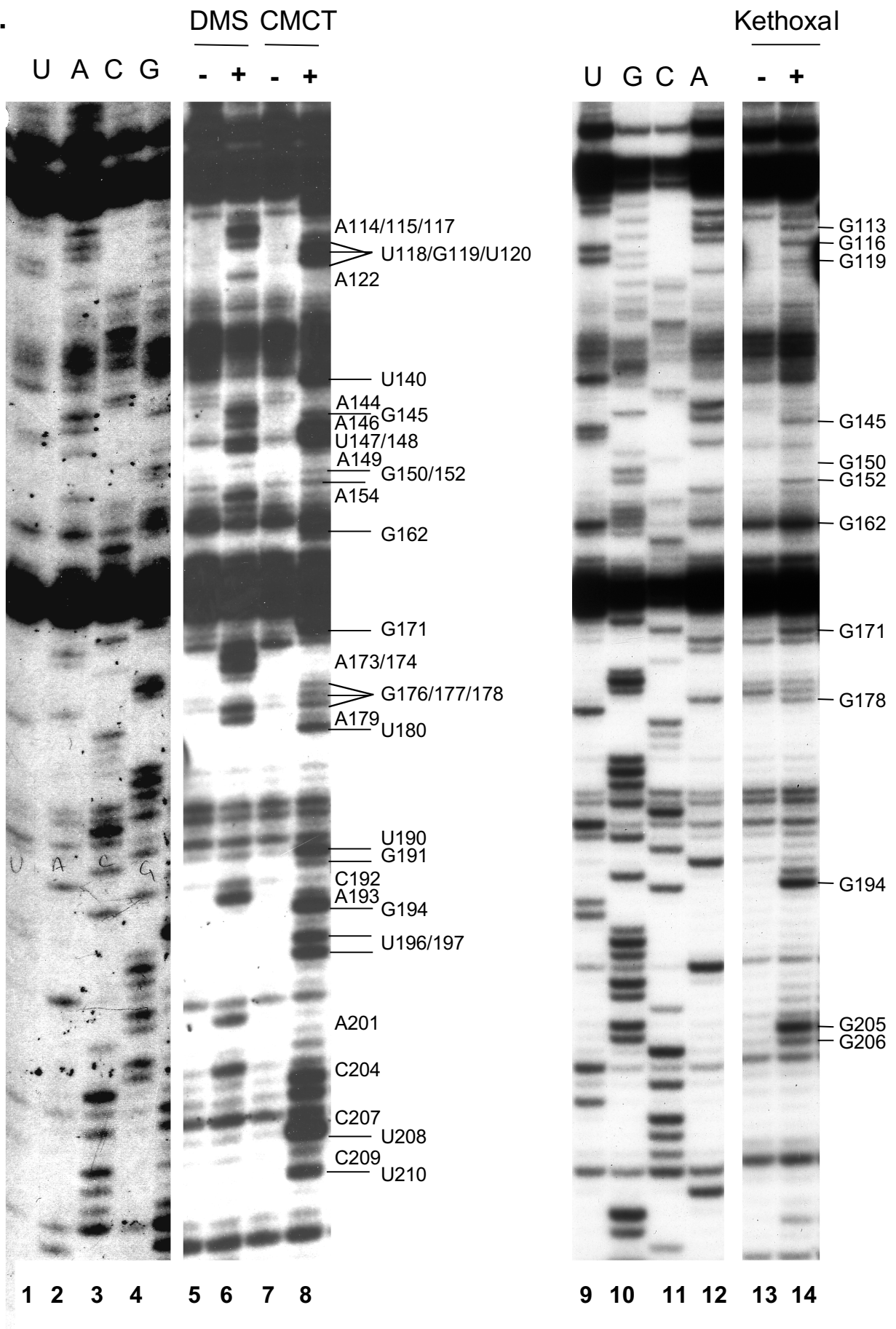


Figure 1, Bonnal et al.

B.



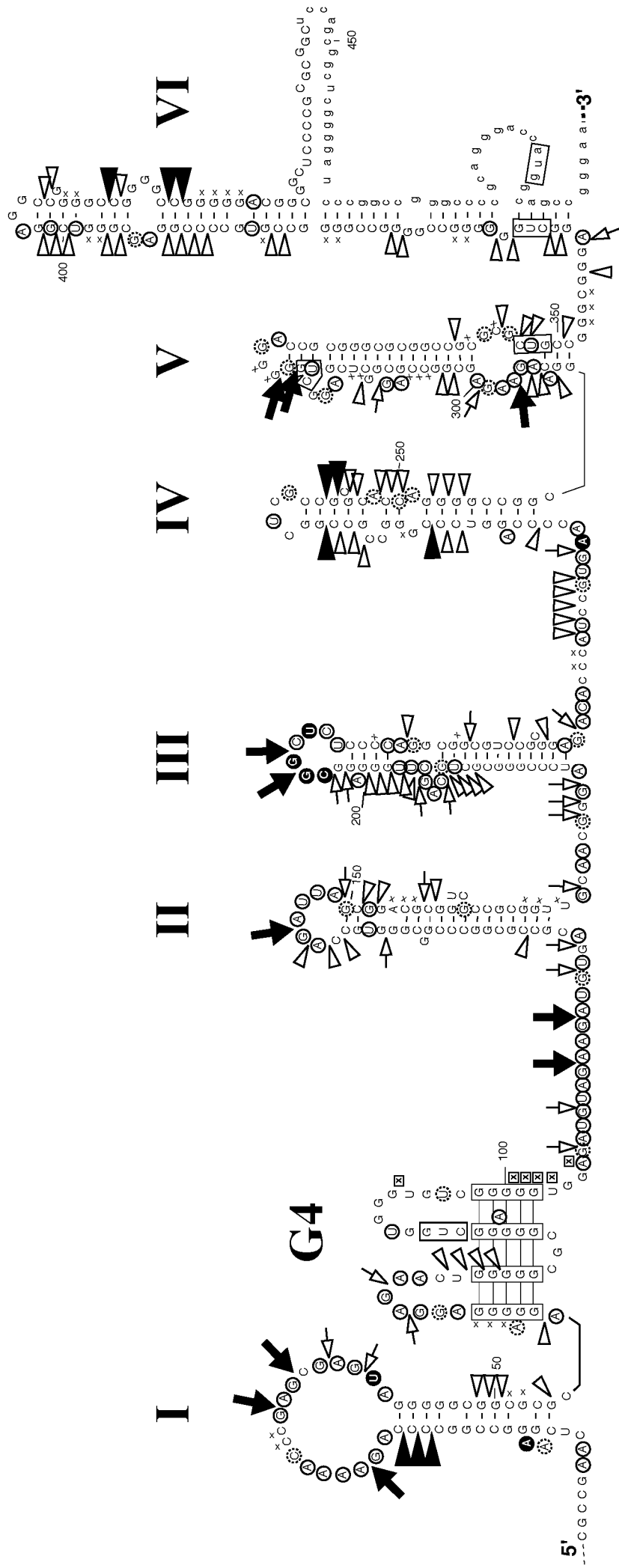
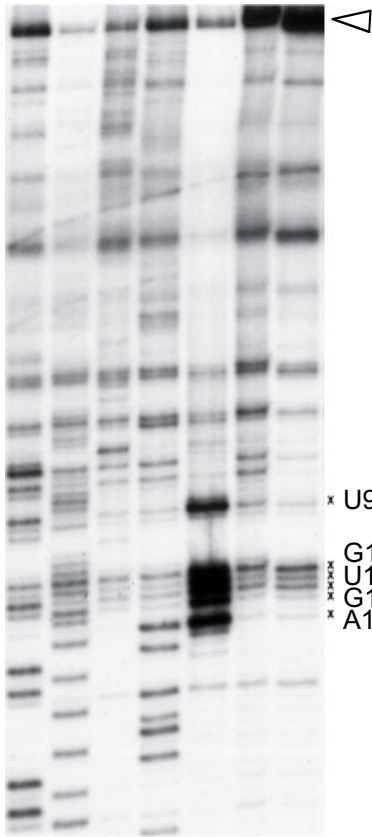


Figure 3, Bonnal et al.

A.

U G C A K NaLi



1 2 3 4 5 6 7

B.

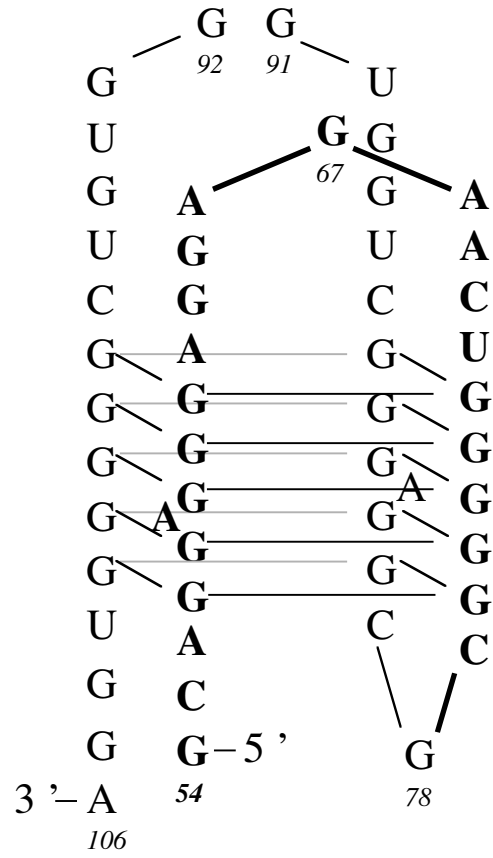


Figure 4, Bonnal et al.

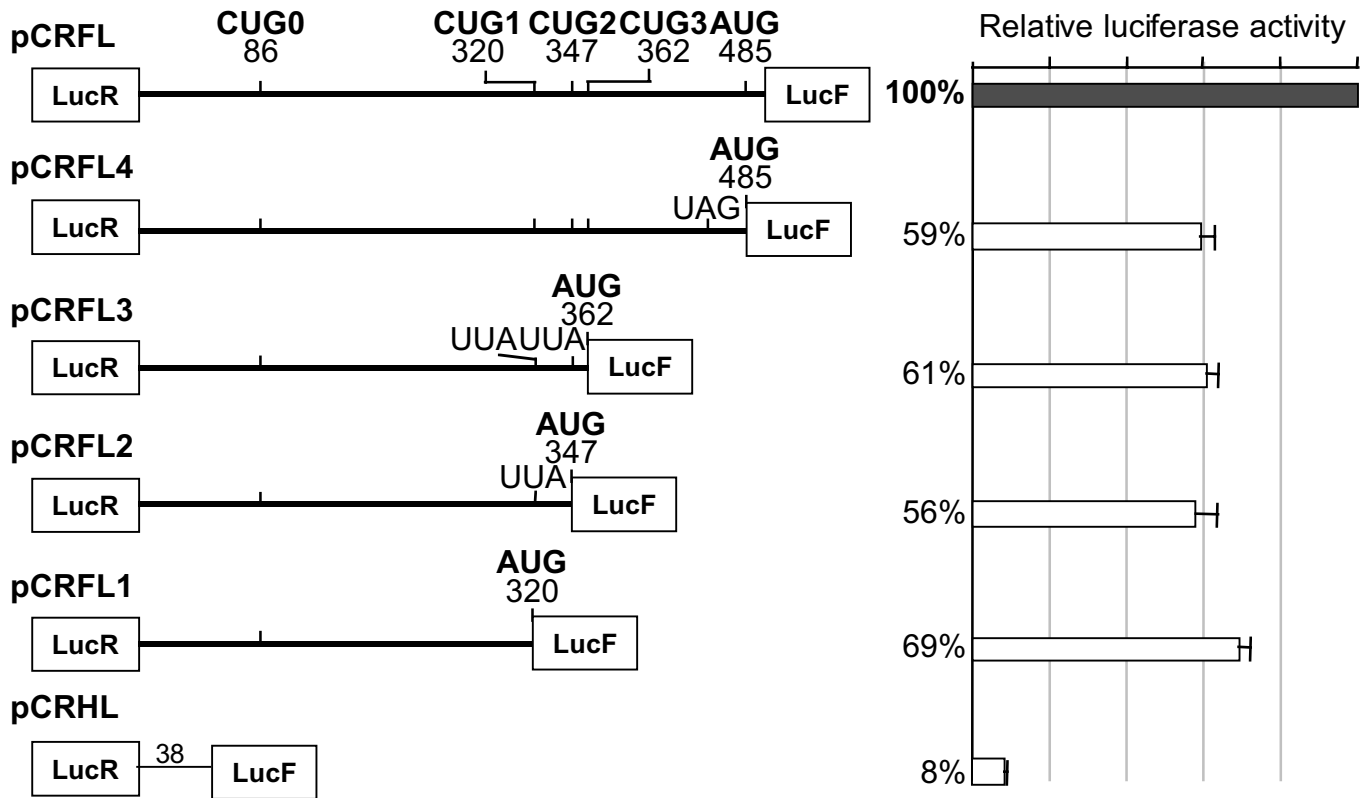
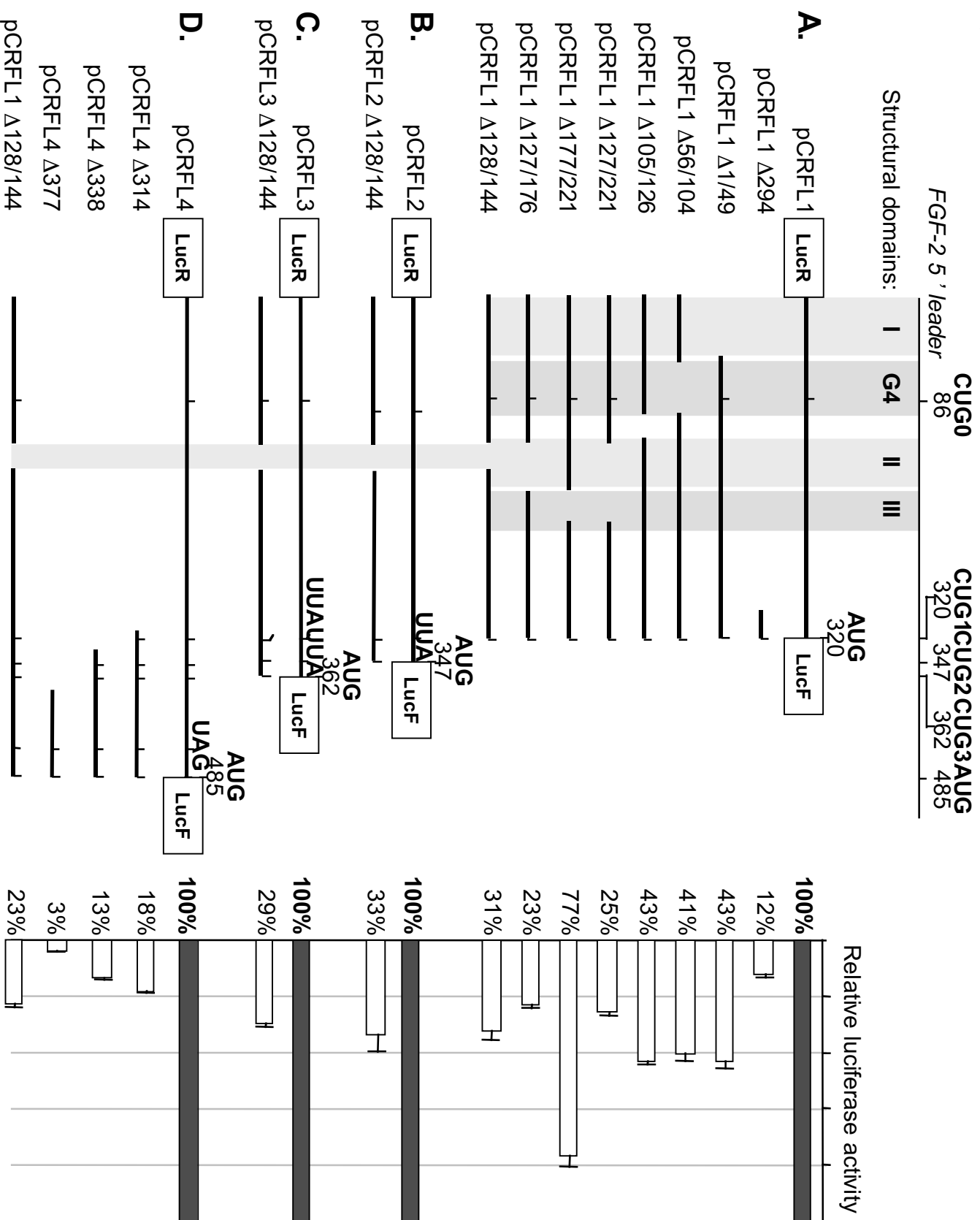


Figure 5, Bonnal et al.



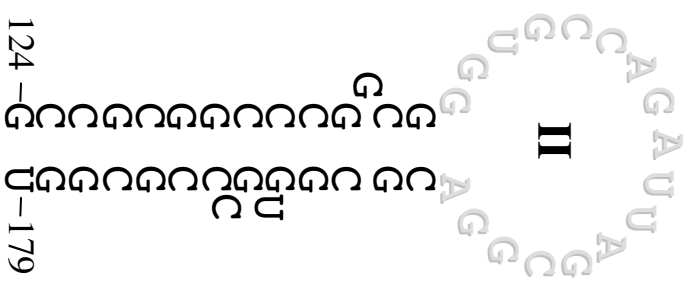
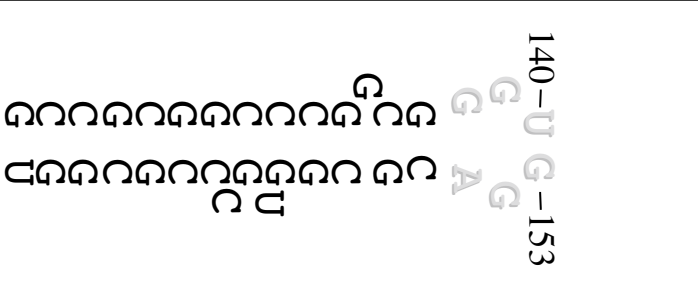

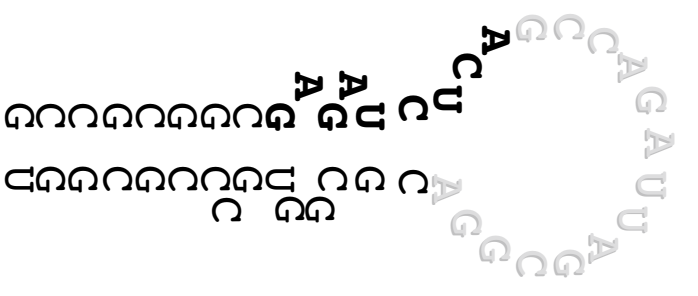
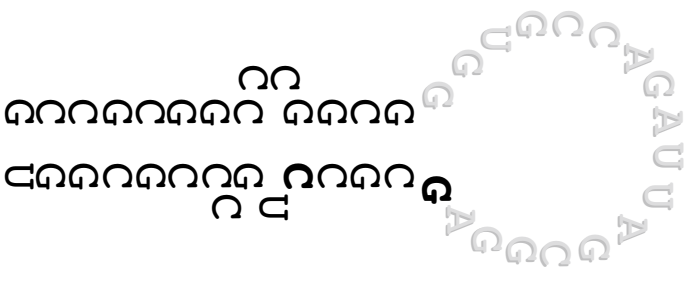
 <p>124-G</p> <p>U-179</p>	<p>140-U</p> <p>153</p> 			
<p>pcRF1</p>	<p>Δ141/152</p>	<p>M142/150</p>	<p>M132/140</p>	<p>M156/160</p>
<p>100%</p>	<p>22% (+/- 0.8)</p>	<p>23% (+/- 0.7)</p>	<p>122% (+/- 8)</p>	<p>111% (+/- 12)</p>

Figure 7, Bonnal et al.

